PCCP

Accepted Manuscript

ROYAL SOCIETY OF CHEMISTRY

www.rsc.org/pccp

Journal Name

RSCPublishing

ARTICLE

Photoinduced Symmetry–Breaking Intramolecular Charge Transfer in a Quadrupolar Pyridinium Derivative

Cite this: DOI: 10.1039/xoxxoooooox

Received ooth January 2012,
Accepted ooth January 2012

DOI: 10.1039/xoxxoooooox

www.rsc.org/

Benedetta Carlotti,*[a] Enrico Benassi,*[b] Anna Spalletti,[a] Cosimo G. Fortuna,[c] Fausto Elisei[a] and Vincenzo Barone[b]

We report here a joint experimental and theoretical study of a quadrupolar, two–branched pyridinium derivative of interest as potential Non–Linear Optical material. The spectral and photophysical behaviour of this symmetric system result greatly affected by the polarity of the medium. A very efficient photoinduced intramolecular charge transfer, surprisingly more efficient than in the dipolar asymmetric analogue, is found to occur by femtosecond resolved transient absorption spectroscopy. TD–DFT calculations are in excellent agreement with these experimental findings and predict large charge displacements in the molecular orbitals describing the ground, and the lowest excited singlet state. The theoretical study revealed also that in highly polar media the symmetry of the excited state is broken giving a possible explanation to the fluorescence and transient absorption spectra resembling those of the one–branched analogous compound in the same solvents. The present study may give an important insight into the excited state deactivation mechanism of cationic (Donor–π–Acceptor–π–Donor)$^+$ quadrupolar compounds characterised by negative solvatochromism, which are expected to show significant Two–Photon Absorption (TPA). Moreover, the water solubility of the investigated quadrupolar system may represent an added value in view of the most promising applications of TPA materials in biology and medicine.

Introduction

Emerging technologies such as imaging, photodynamic therapy, sensing, memory storage, micro– and nano–fabrication are in continuous need for new, highly performing, low cost materials. During the last years chemists are paying increasing attention to organic compounds bearing electron donor (D) and acceptor (A) groups linked by π–conjugated bridges owing to their non–linear optical (NLO) properties. Dipolar (D–π–A) molecules have been extensively investigated,[1–11] whereas the more complex photobehaviour of quadrupolar systems (D–π–A–π–D or A–π–D–π–A) still needs to be deeply understood. An important question to address is the extent of intra-molecular charge transfer (ICT) between D and A groups in these symmetric compounds which can be one of the crucial factors determining the enhanced two–photon absorption (TPA) with respect to their dipolar analogues.[12–17] The study of TPA materials represents one of the hottest topics in today's research due to a great deal of applications[18] (in biology and medicine,[19–23] in optics and optoelectronics,[24,25] in analytical and environmental sciences,[26,27] in optical data storage and micro–fabrication[28–30]) that exploit the advantages of two–photon compared to one–photon processes.

The highly symmetric quadrupolar systems have surprisingly shown, in some cases, spectral and photophysical properties significantly affected by the surrounding medium.[12–14,31] Therefore, for these chromophores the studies carried out up to date suggest the presence of polar electronic states. Recent attempts[32] to model the quadrupolar systems behaviour by means of essential–state calculations led to their classification into three classes, defined considering the bistability of their electronic states: class I–systems characterised by a dipolar excited state; class II–compounds showing stable, non–dipolar states; class III–molecules exhibiting a dipolar ground state. This classification generally implies consequent distinctively different spectroscopic features: positive fluorosolvatochromism for class I, no solvatochromism for class II and negative solvatochromism for class III quadrupolar systems. The most studied class I quadrupolar systems show a lower quadrupolar character coupled with a less important TPA response with respect to the scarcely investigated class II and III ones.

New very interesting frontiers are opened up by the findings of the first ultrafast spectroscopic investigations on quadrupolar systems.[33–35] The results point to an ultrafast localisation of the charge on one branch[36] and to an increased intra-molecular charge transfer (ICT) excited state character when the branching is increased, thus providing a reasonable explanation to the TPA enhancement. However, such results were found only in some neutral quadrupolar systems belonging to the above mentioned class I. Therefore in the framework of the present work we aim to extend the ultrafast spectroscopic investigation to a cationic quadrupolar system. In fact, only a couple of very recent experimental studies on positively charged quadrupolar $(A–\pi–D–\pi–A)^+$ class III polymethine dyes were reported in the literature.[37,38] In this respect, here we aim to carry out a joint experimental and theoretical investigation about the role of ICT in the excited states of a quadrupolar pyridinium derivative taking into account that such a role has been recently emphasised for analogous dipolar cationic compounds.[39,40] The branched quadrupolar compound under study (2,6(*E,E*)–2–[4–(dimethylamino)phenyl]ethenyl–1–methyl–pyridinium **2**, shown in Scheme 1 in comparison with the analogous dipolar system **1**) has a $(D–\pi–A–\pi–D)^+$ structure where the D portions are the electron rich dimethylamino groups and A is the positively charged methyl–pyridinium.

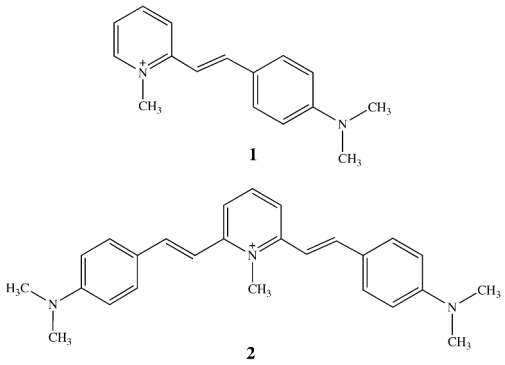

Scheme 1 Molecular structures of compounds **1** and **2**.

Results and discussion

Figure 1 shows the normalised absorption and emission spectra of the quadrupolar compound **2** in comparison with those of the dipolar analogue **1**. In a low polarity solvent, such as dichloroethane (DCE), both the absorption and emission bands of **2** are red–shifted with respect to those of **1**, in agreement with a longer conjugated system. Moreover, as expected for an angular meta substituted compound where the two arms act as almost separate chromophores,[41] the extinction coefficient of the quadrupolar system is nearly doubled compared to that of the dipolar one (for example in $CHCl_3$ $\varepsilon_1(\lambda_{max})$=39700 $M^{-1}cm^{-1}$ and $\varepsilon_2(\lambda_{max})$=66000 $M^{-1}cm^{-1}$). However, a very peculiar behaviour is observed for **1** and **2** in a highly polar solvent, such as water (W). Whereas a significant bathochromic shift of the absorption band still occurs on going from the dipolar to the quadrupolar structure, the two emission bands roughly overlap.

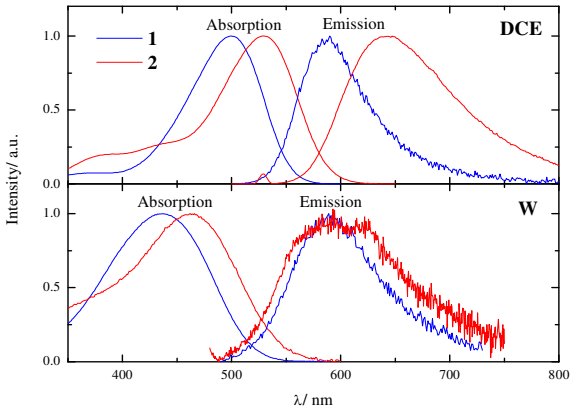

Figure 1 Normalised absorption and emission spectra of compound **1** (blue) and **2** (red) in DCE (upper panel) and W (lower panel).

Despite the symmetry of the molecular structure, the spectral properties of **2** are significantly affected by the polarity of the solvent. The absorption band is noticeably moved toward the blue (from 530 nm in dichloromethane (DCM) to 464 nm in W) by the increase in solvent polarity (Table 1 and Figure 2A), similarly to what already observed for the dipolar analogous compound **1**.[40] A strong enlargement of the absorption band is observed with increasing solvent polarity (Full Width Half Maximum, FWHM, from 2985 cm^{-1} in DCM to 6175 cm^{-1} in W) together with a significant decrease of the molar extinction coefficient of **2** on going from $CHCl_3$ (66000 $M^{-1}cm^{-1}$) to W (45000 $M^{-1}cm^{-1}$). These experimental findings (shift, broadening [42,43] and intensity decrease of the absorption band in the more polar media) may be a hint of the charge transfer nature of the considered transition (further evidences are furnished by the theoretical calculations, *vide infra*). An unbiased analysis of solvent shifts requires, in our opinion, comparison of a large panel of different solvents. Those employed in this study can be categorised into three different classes, namely: (i) chlorinated solvents; (ii) protic solvents; (iii) non–protic and non–chlorinated solvents. Within each solvent class, the solvatochromic shifts observed for the absorption band of **2** show a correlation with solvent polarity (see Table 1 and Supporting Information, Figure S1). Some small effects due to H-bonding interactions may be present for such a molecular system bearing two dimethyl amino groups, mainly in the highly protic water. When considering the cases of the alkane chloride and protic solvents together, the correlation with solvent polarity is still observable. This trend closely parallels that previously reported for another methyl–pyridinium derivative[44] and suggests that, besides electrostatic interactions, dispersive contributions could play a role for non–protic and non-chlorinated solvents. Our spectral results are in fair agreement with those previously reported for **2** in few, scattered solvents.[45–47] As observed for **1**,[40] no evidence of ionic pairs emerged in the considered *media* and thus the obtained electronic properties can be ascribed uniquely to the cation.[48] The solvatochromic shifts are hazardous to

rationalise according to simple models described in the literature considering the contributions of the various solute – solvent interactions because of the complex nature of the system under study. Aware of the limitations of simple electrostatic models for our system, anyhow we have attempted to provide a qualitative explanation of its behaviour (see Supporting Information and Table S2). The dipole moment for a charged species is undefined since it depends on the choice of the coordinate origin. However, in Quantum and Computational Chemistry, a "working definition" is always assumed, which refers to the centre of the nuclear charges of the system (which in our case is practically coincident with the centre of mass).[49] However, the computed electric properties of the system **2**, unlike **1**, lead us to suppose that the contribution to the solvatochromic effect due to the electric dipole moment should not be particularly significant because of the molecular symmetry. In fact, regardless of the solvent, small electric dipole moment in the ground state resulted from the calculations (ca. 0.9 D see Supporting Information, Table S1; nonzero values are obtained because of the bent structure of compound **2**, which actually is not a pure quadrupole as arises from Scheme 1) and a small increase of the electric dipole moment with no orientation change is foreseen when going from S_0 to the adiabatic S_1 state. The results obtained from our tentative rationalisation of the solvatochromic shifts indicate that the negative solvatochromism is probably related to the monopole contribution[50] and also to a substantial change in the quadrupole moment[51] (see Supporting Information, Table S1) when going from the ground to the first excited singlet state.

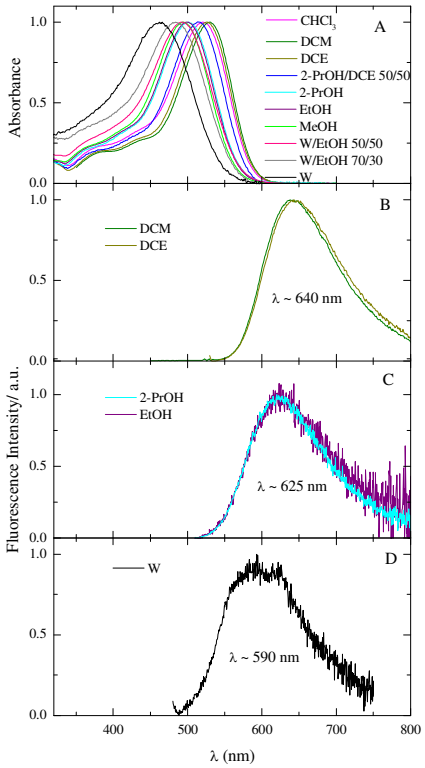

Figure 2 Normalised absorption (A) and emission (B, C, D) spectra of **2** in solvents of different polarity.

On the contrary, solvent effects on the emissive behaviour of **1** and **2** are quite different, the emission band of the former compound showing a negligible dependence on solvent polarity (for instance in the case of **1**: λ_{max}= 590 nm in DCM, 589 nm in EtOH and 589 nm in W).[40] The emission spectrum for the quadrupolar system **2** (Figure 2) is centred around 640 nm in the lower polarity solvents (panel B), around 620 nm in the polar media (panel C) and at 590 nm in the highly polar W (panel D). Therefore, in aqueous solution a net hypsochromic shift of 50 nm was observed, responsible for a fluorescence profile similar to that observed for the dipolar compound **1** in the same *medium*.

To gain further insight into the reason originating this particular behaviour of the emission of **2** in polar *media*, a comprehensive computational investigation was carried out about the structural and electronic properties of **2** both *in vacuo* and in solution. The geometries of the S_0 and S_1 states for the most stable rotamer were optimised by methods rooted into the Density Functional Theory (DFT) and its time dependent (TD-DFT) extension *in vacuo* and in implicit solvents chosen in order to explore a wide range of polarisation effects. Although multi-reference and vibronic effects could be important for a quantitative reproduction of spectra, adiabatic transition energies computed by hybrid density functionals are usually sufficient for a semi-quantitative comparison with experimental trends in the absence of extreme charge-transfer effects.[52,53] The optimised geometries in a low polar (DCM) and a highly polar (MeCN) solvent are shown in Figure 3. The geometries of both the ground and the first excited state calculated in DCM (very close results are obtained *in vacuo*) have a $\mathbf{C}_{2v}$ symmetry; the atoms belonging to the central ring are almost co–planar and this is also the case for the atoms of both the dimethylaminostyryl moieties. The two lateral moieties form dihedral angles of about 160 degrees with the pyridinium ring (see Supporting Information, Table S3). In MeCN a stronger distortion from co–planarity is found in the still symmetrical S_0 geometry (dihedral angles of about 145 degrees), whereas the symmetry of the system is completely broken in the S_1 geometry. In this case one of the arms is co–planar with the pyridinium (dihedral angle around 180 degrees) whereas the other is almost perpendicular (dihedral angle 108 degrees).

The electronic properties of **2** are calculated considering both the S_0 and the S_1 optimised geometries: the plots of the frontier molecular orbitals (MOs) are shown in Figure 4 in DCM and MeCN, as an example. In particular, the lowest excited singlet state S_1 is mainly described by the HOMO – LUMO transition of π,π^* nature in all cases. When considering the ground state optimised geometry, both in DCM and in MeCN, the HOMO → LUMO transition implies a symmetrical charge displacement from the lateral electron rich dimethylamino groups toward the central electron deficient methyl–pyridinium (difference of electron density between ground and first excited singlet state and Mulliken charge analysis, shown in Supporting Information, Tables S4 and S5, give additional information about the charge movement occurring during the $S_0 \rightarrow S_1$ transition). When the geometry is optimised for the S_1 state, the

molecular orbitals are very similar in DCM (additionally, the difference of the electron density for the emission transition is shown in Supporting Information, Figure S2). The Mulliken charge analysis (Table S5) clearly indicates that an important charge redistribution (symmetrical back electron transfer toward the dimethyl amino groups) takes place on going from the Frank-Condon to the fully relaxed excited singlet state, in agreement with the experimental findings of the ultrafast transient absorption measurements (*vide infra*). The emitting species in DCM is therefore characterised by a quasi−planar geometry (Figure 3) and is described by molecular orbitals distributed on the whole molecular structure (Figure 4). On the contrary, S_1 looks like a symmetry−broken state in MeCN where a very significant charge displacement occurs from one branch to the other of the molecular structure. These findings issuing from quantum mechanical (QM) calculations provide a possible explanation for the peculiar solvent dependent behaviour of the emission spectrum of **2**. In fact, in polar *media* the molecular orbitals involved in the emission transition (LUMO−HOMO) are localised each only on one branch of the quadrupolar system, which in this case becomes the fluorescent portion of the system being similar to that involved in the emission of the single−arm **1** molecule. The computational investigation performed also for the $S_0 \rightarrow S_2$ transition (see Supporting Information, Table S4) shows some charge transfer character, but the much lower oscillator strength with respect to the $S_0 \rightarrow S_1$ one makes it less important in describing the experimental spectral properties of compound **2**.

The computational predictions of the spectra and the investigation of the singlet excited state nature are performed in different solvents after S_0 and S_1 geometry optimisation (see the results collected in Table 1). In all cases, the theoretically predicted absorption and emission spectra are in excellent agreement with their experimental counterparts. The remarkable results obtained by employing an implicit polarisable representation of the solvent (CPCM) suggests that hydrogen bond interactions do not play a major role in tuning solvatochromic spectral shifts.

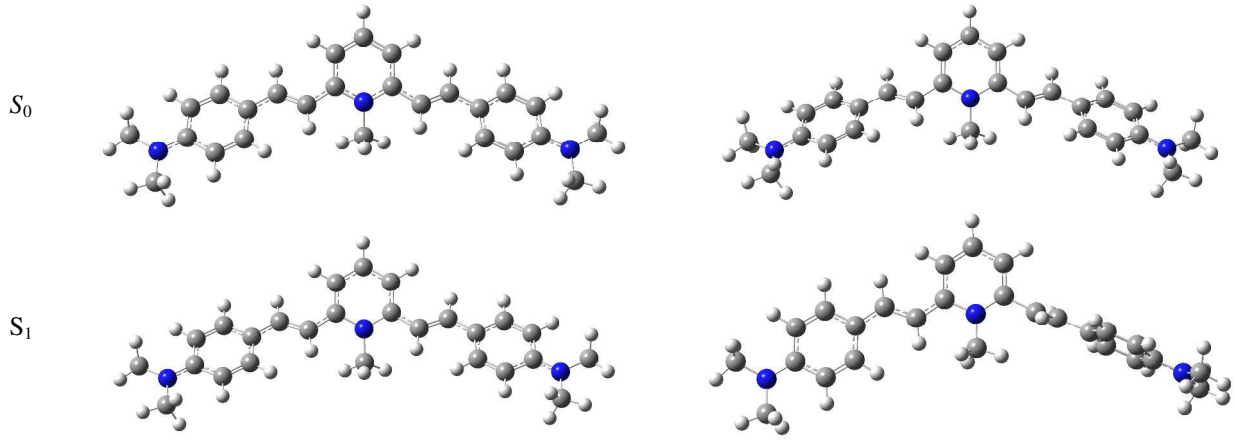

Figure 3 Comparison between the S_0 and S_1 optimised geometries in DCM and in MeCN.

Table 1 Spectral and photophysical properties of compound **2** in solvents of different polarity belonging to the three classes (typed with different characters; see main text).

		Experimental					Theoretical			
solvent	f (ε, n^2)[b]	λ_{abs}/nm	λ_F/nm	Δν/cm^{-1}	ε/(M^{-1}cm^{-1});f_{01}	ϕ_F	λ_{abs}/nm	λ_F/nm	f_{01}	f_{10}
$CHCl_3/CCl_4$ (50/50)	**0.201**	**519**	**620**	**3140**						
$CHCl_3$ [a]	**0.296**	**521**	**628**	**3230**	**66000;1.45**	**0.17**	**521**		**1.72**	
THF	0.420	499	646	4520			499		1.77	
DCM [a]	**0.437**	**530**	**647**	**3380**		**0.10**	**534**	**646**	**1.78**	**1.80**
DCE	**0.445**	**526**	**647**	**3630**		**0.04**	**527**		**1.56**	
DMSO	0.527	495	621	4100		0.001	495		1.84	
2−PrOH	*0.552*	*501*	*625*	*3960*		*0.017*	*502*		*1.53*	
Ac	0.570	492	630	4450		0.0006	493		1.87	
EtOH	*0.577*	*499*	*625*	*4040*		*0.004*	*500*		*1.88*	
W/EtOH (30/70)	*0.608*	*496*	*610*	*3770*						
MeCN [a]	0.611	490	608	3960		0.0003	490	607	1.88	0.086
MeOH	*0.617*	*494*	*618*	*4060*		*0.001*	*494*		*1.83*	
W/EtOH (50/50)	*0.620*	*493*	*612*	*3940*		*0.0009*				
W/EtOH (70/30)	*0.629*	*483*	*595*	*3900*						
W (pH=5) [a]	*0.640*	*464*	*590*	*4600*	*45000;1.40*	*0.0001*				

[a] negligible $\phi_{tt\rightarrow ct}$; [b] $f(\varepsilon,n^2)=[2(\varepsilon-1)/(2\varepsilon+1)]-[2(n^2-1)/(2n^2+1)]$. In bold data referring to chlorinated solvents; in Italics data referring to protic solvents.

Journal Name RSCPublishing

ARTICLE

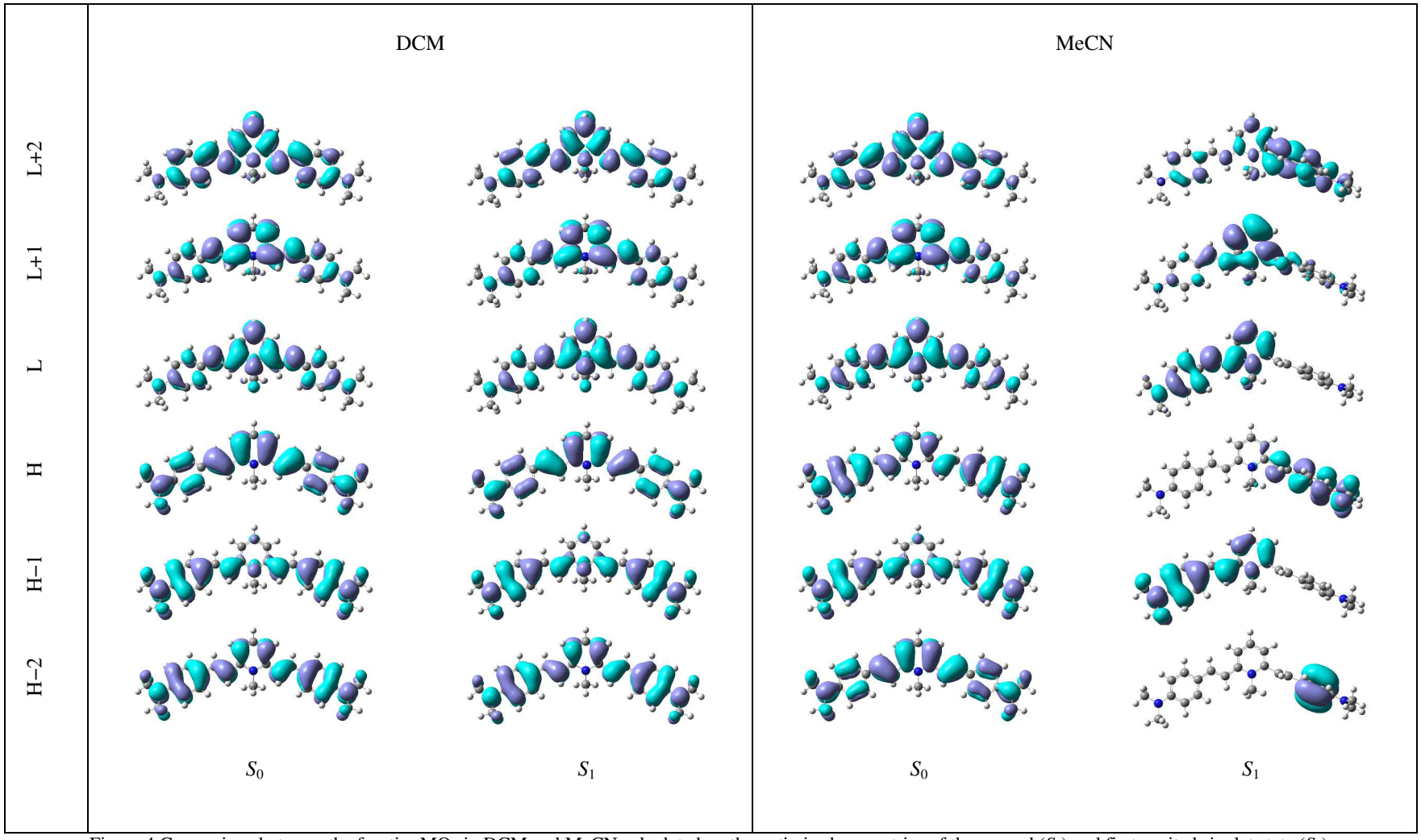

Figure 4 Comparison between the frontier MOs in DCM and MeCN calculated on the optimised geometries of the ground (S_0) and first excited singlet state (S_1).

Journal Name RSCPublishing

ARTICLE

The photophysical behaviour of **2** is also significantly tuned by solvent effects. In particular, the fluorescence quantum yield is strongly depressed when increasing the solvent polarity, the decrease reaching three orders of magnitude when going from $CHCl_3$ to W (Table 1). This behaviour is usual for push–pull compounds, but here the effect is surprisingly more evident in the case of the symmetric compound **2** with respect to the two orders of magnitude decrease of ϕ_F observed for the asymmetrical molecule **1** (ϕ_F=0.14 in DCM and 0.001 in W for this latter).[40] The significant reduction of the fluorescence in the more polar solvents is interpreted considering the geometry predicted for the emitting excited state in these *media* (Figure 3): twisted geometries are known to show preferentially non radiative decay pathways. and to deactivate mainly by internal conversion (IC) The occurrence of (*trans*, *trans*) → (*trans*, *cis*) photoisomerisation of **2** was investigated in some solvents (chosen with the aim of covering a large polarity interval, see Table 1) and in all cases it was found to be negligible. Being also the intersystem crossing efficiency always very low (see below), the deactivation pathways operative for **2** in the low polarity solvents are fluorescence and IC whereas this latter becomes the unique decay process in the more polar solvents where an important fluorescence quenching occurs.

To gain further insight into the observed spectral solvatochromism and the fluorescence quenching upon increasing solvent polarity, the dynamics of the excited states of **2** was investigated by femtosecond resolved transient absorption. Figure 5 shows a contour plot of the experimental data (panel A) and the main time–resolved absorption spectra and kinetics recorded at significant wavelengths (panel B), together with the spectral and kinetic properties of the main components obtained by Singular Value Decomposition and Target Analysis[54] (panel C) for **2** in MeOH. Table 2 shows the results obtained in different solvents, *viz.* the lifetime τ and the spectral shape of each detected transient. The time–resolved spectra show the tail of the ground state bleaching (below 540 nm), a stimulated emission band significantly red–shifting in time and a positive transient absorption signal centred around 570 nm, which was formed and subsequently decayed. Both the Global and the Target Analysis revealed the presence of three components with lifetimes of 0.31, 3.0 and 10 ps. The bathochromic shift of the stimulated emission in time and the values of the two shorter lifetimes are a signature of the occurrence of solvent relaxation following the excitation of **2** in MeOH. In fact, solvation is known to show a time–dependence which is biexponential concerning both the inertial and diffusive part of the response.[55] The lifetimes of 0.3 and 3.0 ps obtained from the global fitting can be therefore assigned to the inertial and diffusive solvation in MeOH. The longer living component of 10 ps can be associated to the relaxed lowest excited singlet state.

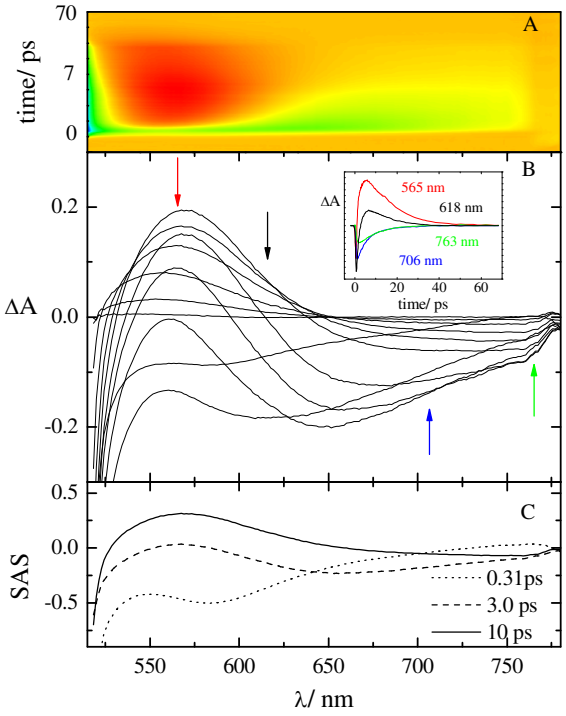

Figure 5 Pump–probe absorption spectroscopy of **2** in MeOH (λ_{exc}=400 nm): A) contour plot of the experimental data, B) time resolved absorption spectra recorded 0.2, 0.6, 1.0, 1.5, 2.5, 5.9, 8.7, 12, 19, 29 and 54 ps after the laser pulse. Insets: decay kinetics recorded at meaningful wavelengths and C) Species Associated Spectra (SAS) of the decay components obtained by Target Analysis.

Similar results were found from the measurements carried out in other solvents and summarised in Table 2. The only significant exception is the case of $CHCl_3$, the lowest polar investigated solvent. In fact, among the three components evidenced by the global fitting (characterised by lifetimes of 2, 20 and 180 ps, respectively) only the fastest one is compatible with the occurrence of solvation in this *medium*.[55] Both the second and the third component show rather long lifetimes, which are not ascribable to the solvation dynamics. The 20 ps component was assigned to the locally excited state ($^1LE^*$), the state reached by light absorption, whereas the 180 ps component is due to an intramolecular charge transfer state ($^1ICT^*$). Even thought the 400 nm excitation employed for the ultrafast spectroscopic investigation implies that the S_2 state is initially reachable by light absorption in all the investigated solvents (see Supporting Information, Table S4), the much lower oscillator strength of the transition to S_2 suggests that the

major part of the exciting photons are absorbed to produce the S_1 state. In any case, the $S_2 \rightarrow S_1$ internal conversion should occur very fast.[56] Therefore, the $^1LE^*$ intermediate detected for **2** only in the lowest polar *medium* probably corresponds to a competitive species in the S_1 state (lying in a relative minimum of the potential energy surface), whose stability is substantially modulated by the solvent polarity and that in $CHCl_3$ evolves in tens of ps to produce the fully relaxed $^1ICT^*$ state.

Table 2 Excited states lifetimes of **2** in solvents of different polarity (obtained by transient absorption upon excitation at 400 nm).

Solvent	τ/ ps	λ/ nm	Transient
$CHCl_3$	2	<720(–), >720(+)	Solv.(d)
	20	580(+), 670(–)	$^1LE^*$
	180	590(+), 710(–)	$^1ICT^*$
DCM	0.50	<735(–), >735(+)	Solv.(i)
	1.80	580(+), 660(–)	Solv.(d)
	180	585(+), 685(–)	$^1ICT^*$
DCE	1.0	<775(–), >775(+)	Solv.(i)
	4.3	585(+), 660(–)	Solv.(d)
	220	600(+), 695(–)	$^1ICT^*$
DMSO	0.43	615(–)	Solv.(i)
	3.7	575(+), 675(–)	Solv.(d)
	11	570(+), >720(–)	$^1ICT^*$
Ac	0.1	595(–)	Solv.(i)
	0.99	510(–), 690(–)	Solv.(d)
	8.9	<530(–), 570(+), 760(–)	$^1ICT^*$
MeCN	0.21	630(–)	Solv.(i)
	0.60	<550(–), 585(+), 745(–)	Solv.(d)
	6.1	<520(–), 560(+), 760(–)	$^1ICT^*$
EtOH	0.82	580(–)	Solv.(i)
	6.7	565(+), 650(–)	Solv.(d)
	31	570(+), 710(–)	$^1ICT^*$
MeOH	0.31	<540(–), 580(–), 765(+)	Solv.(i)
	3.0	<550(–), 565(+), 655(–)	Solv.(d)
	10	<530(–), 570(+), 745(–)	$^1ICT^*$
W/MeOH 90/10	0.36	590(–)	Solv.
	5.1	530(+), 630(–)	$^1ICT^*$

Spectral properties refer to Species Associated Spectra (SAS) calculated by Target Analysis. The symbols (+) and (–) stand for positive and negative signals, respectively. Solv.(i)=Inertial Solvent Relaxation; Solv.(d)=Diffusive Solvent Relaxation.

The ICT process, detected for **2** in $CHCl_3$, occurs more efficiently in the more polar solvents, the $^1LE^* \rightarrow {}^1ICT^*$ transition becoming faster than solvation in these cases. Also, upon increasing the solvent polarity a shortening of the $^1ICT^*$ lifetime is observed (at least when solvents of the same nature are compared: the polar and aprotic DMSO, Ac and MeCN, the polar and protic EtOH, MeOH and W), this trend being parallel to the one observed for the fluorescence quantum yield in the various solvents. In fact, a decrease of more than one order of magnitude is observed for the radiative rate constant with the solvent polarity (k_F=5.6×10^8 s^{-1} in DCM, 0.49×10^8 s^{-1} in MeCN and 0.20×10^8 s^{-1}in W); this behaviour parallels the solvent dependence of the oscillator strength for the $S_1 \rightarrow S_0$ transition resulting from the calculations (f_{10} in Table 1) and pointing to an increased ICT character accompanied by formation of a twisted conformation of the emitting state (TICT) in the more polar *media*.

In the case of the dipolar analogue **1** a similar behaviour is evidenced by the ultrafast spectroscopic investigation (data from ref. 40 are summarised in Supporting Information, Table S7), revealing an interesting competition between ICT (the rate controlling step in low polarity solvents, *i.e.* $CHCl_3$ and DCM) and solvation (the rate controlling process in all the high polarity solvents).[40] However, the differences that are present in the excited state dynamics of the two systems are revealing. In fact, in DCM the $^1LE^* \rightarrow {}^1ICT^*$ transition, which was slow for **1**, becomes faster and solvation controlled in the case of **2**. This peculiar finding indicates that ICT is faster and more efficient in the symmetric quadrupolar system than in the asymmetric dipolar analogue. Moreover, the time constant of the $^1ICT^*$ state was shorter in the more polar solvents for the quadrupolar with respect to the dipolar system in the same *media* (for example in MeOH τ ($^1ICT^*$) is 24 ps for **1**[40] and 10 ps for **2**, respectively), pointing to a stronger ICT (or TICT) character of this state in the branched compound, in agreement also with its decreased fluorescence efficiency.

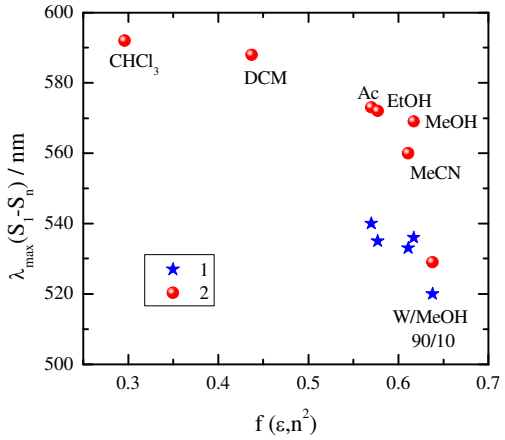

Figure 6 Maxima of the absorption spectra of the longer living component (the lowest excited singlet state with an ICT character) obtained for compound **1** (blue) and **2** (red) in various solvents of different polarity (f (ε, n^2)) from the Target Analysis of the femtosecond transient absorption data.

The Target Analysis associates to the $^1ICT^*$ state of **2** a spectral shape characterised by a positive absorption band which is blue–shifted upon increasing the solvent polarity, being centred at 590 nm in the lower polar solvents ($CHCl_3$ and DCM), at 570 nm in the polar *media* (Ac, DMSO, MeCN, EtOH, MeOH) and at 530 nm in the highly polar W/MeOH 90/10 mixture (see Table 2 and Figure 6). The absorption maximum for the relaxed lowest excited singlet state of **2** is well reproduced by the QM calculations carried out in DCM and MeCN and is associated to a $^1ICT^* \rightarrow S_2$ transition (see Supporting Information, Table S8). The hypsochromic shift of this band brings the $^1ICT^*$

absorption of **2** to a position very close to that typical of the $^1ICT^*$ for **1** (which absorbs at 535 nm in the polar *media* and at 520 nm in W/MeOH 90/10, see Figure 6 and Supporting Information, Figure S3), confirming the symmetry–breaking occurrence in the higher polar *media* previously observed for the $S_1 \rightarrow S_0$ emission spectrum in W (Figure 1).

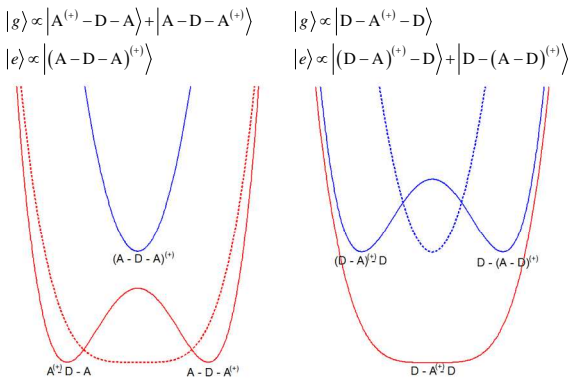

Scheme 2 Sketch of the ground (red) and excited (blue) electronic states in low polar (dashed) and polar (solid) solvents of cationic $(A\text{-}D\text{-}A)^+$ (left) and $(D\text{-}A\text{-}D)^+$ (right) quadrupolar systems showing symmetry breaking.

The concept of symmetry–breaking was proposed for the first time about seven years ago by Terenziani *et al.*[32] in order to explain the behaviour of solvatochromic quadrupolar compounds. The cases of some cationic quadrupolar systems belonging to the so–called class III, investigated more recently by the same author,[37,38] can be examplified as $(A–D–A)^+$, so that, within a Valence-Bond (VB) picture, the ground state can be described by two limit resonance structures, where the positive charge tends to be localised on one of the two acceptor chromophores, *viz.* $(A^{(+)}–D–A) \leftrightarrow (A–D–A^{(+)})$, especially when the solvent is highly polar (see Scheme 2, left panel). Therefore, for those systems, the symmetry–breaking phenomenon manifests itself in the ground state (in highly polar *media*), whereas in the excited state the symmetry is restored, since, due to the interaction with the photon, the charge is probably delocalised on the whole structure, *viz.* $(A–D–A)^+$. On the contrary, the pyridinium derivative under study in this work is the first case of a positively charged quadrupolar system showing negative solvatochromism, where the opposite behaviour is observed. Here we are faced with two donor chromophores and one single acceptor, $(D–A–D)^+$. So, within the same VB picture (see Scheme 2, right panel), in the ground state, the positive charge tends to be localised on the central molecular moiety, *viz.* $(D–A^{(+)}–D)$, and thus the structure is symmetrical. Upon electronic excitation, the charge tends to localise on one of the two arms, leading to two limit resonance structures, $(D–A)^{(+)}–D \leftrightarrow D–(A–D)^{(+)}$, which, in turn, generate symmetry–breaking in the excited state. This simple VB picture allows an interpretation of our experimental and theoretical results and suggests that we are dealing with a singular case of class I quadrupolar system (featured by a bistable excited state) showing a peculiar solvatochromic behaviour. A similar VB model can be also applied to neutral molecules with A–D–A or D–A–D features, when considering partial charges instead of net charges. In fact, symmetry breaking was invoked to explain the experimental findings of Goodson III *et al.*.[33,34] about the excited state dynamics of neutral class I quadrupolar molecules. To the best of our knowledge, this is the first time the phenomenon of excited state symmetry–breaking is effectively detected in a cationic quadrupolar system by a combined experimental and theoretical study.

The triplet properties were characterised by means of nanosecond resolved laser flash photolysis. The signal recorded by direct laser excitation of **2** is rather low in all the investigated solvents, with an intersystem crossing (ISC) quantum yield of 0.042 in DCM and even lower in MeCN (Table 3). The triplet absorption spectrum, measured producing the triplet of **2** in MeCN by sensitisation with a high energy triplet donor (benzophenone), is shown in Figure 7. It exhibits a main band at 620 nm and a secondary band at 870 nm, both bathochromically shifted with respect to those observed for **1** in the same solvent (Table 3).

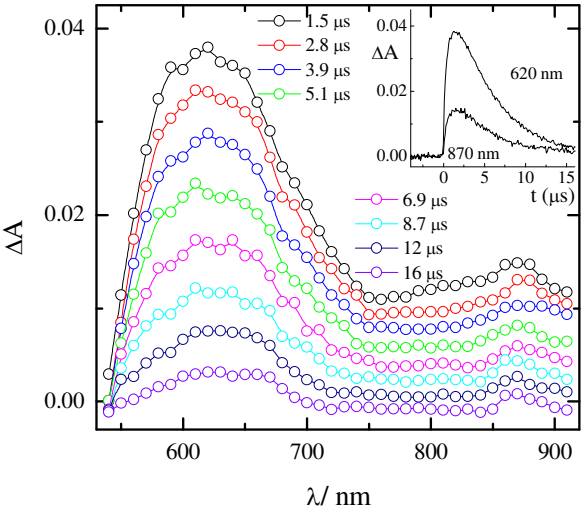

Figure 7 Transient absorption spectra of **2** in MeCN sensitised by benzophenone recorded at different delays after the laser pulse (λ_{exc}=355 nm). Insets: decay kinetics recorded at meaningful wavelengths.

Table 3 Triplet properties of **1** and **2** in DCM and MeCN (λ_{exc}=355 nm, ns resolution).

Comp.	Solv.	λ_{max}/nm	τ_T/µs	ε_T/($M^{-1}cm^{-1}$)	ϕ_T
1[40]	DCM	600,860	1.6		0.27
	MeCN[a]	590,840	7.9	20100	0.008
2	DCM		4.7		0.042
	MeCN[a]	620,870	5.0	15600	<0.005

[a] sensitised by benzophenone

The reason underlying the observed low ISC and photoisomerisation efficiencies of **2** (in fact, in the case of **1** the triplet production is significant in DCM and accompanied by a substantial photoreactivity following a triplet mechanism in this

low polar *medium*)[40] was investigated with the aid of QM calculations. The energy and nature of the lowest singlet and triplet excited states for **1** and **2** in DCM were obtained and are shown in Figure 8. In the case of **1**, there are two triplet states lying at similar or lower energy than S_1. The T_2 state is particularly interesting because it is very close to S_1 and is mainly described by a HOMO → LUMO+1 transition, which involves a molecular orbital mainly localised on the pyridinium. The $S_1 \rightarrow T_2$ transition should be involved in the efficient ISC process of **1** in DCM ($k_{ISC}=2\times10^9$ s^{-1}), which looses its efficiency in the polar MeCN solvent where the competitive IC is the deactivation pathway responsible for all the absorbed photons.[40] In the case of **2**, there are three triplet states placed at close or lower energy with respect to S_1 in DCM (Figure 8, right panel). However, none of them shows a peculiar nature and therefore should give an important spin–orbit coupling with the lowest excited singlet, determining an ISC (and a consequent possible *trans–cis* photoisomerisation *via* triplet state) that in this case is never efficient ($k_{ISC}=1.8\times10^8$ s^{-1} for **2** in DCM).

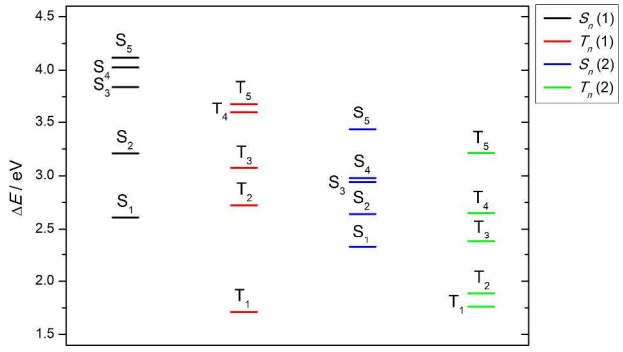

Figure 8 Comparison between the first five singlet and triplet excited electronic states in DCM for compound **1** (left) and **2** (right). For **1**: S_1 mainly H → L; T_2 mainly H → L+1; T_1 mainly H → L (see Supporting Information, Figure S4); for **2**: S_1 mainly H → L; T_3 and T_2 mainly H−1 → L and H → L+1; T_1 mainly H → L (see Figure 3).

Experimental

Materials: Compound **2** was synthetised as iodide salt following the procedure described in a previous work[57]. Measurements were performed in various organic solvents of spectroscopic grade from Sigma–Aldrich and used without further purification: chloroform ($CHCl_3$), carbon tetrachloride (CCl_4), dichloromethane (DCM), dichloroethane (DCE), acetone (Ac), dimethylsulfoxide (DMSO), acetonitrile (MeCN), 2–propanol (2–PrOH), ethanol (EtOH), methanol (MeOH), water (W).

Photophysical measurements: A Perkin–Elmer Lambda 800 spectrophotometer was used for the absorption measurements. The fluorescence spectra were measured by a Spex Fluorolog–2 F112AI spectrofluorimeter.

Triplet formation quantum yields and lifetimes (ϕ_T and τ_T) were measured by a nanosecond laser flash photolysis setup previously described (Nd:YAG Continuum, Surelite II, third harmonics, λ_{exc} = 355 nm, pulse width ca. 7 ns and energy ≤ 1mJ $pulse^{-1}$).[58,59]

A detailed description of the experimental setup for ultrafast spectroscopic and kinetic measurements has already been reported.[60,61] The 400 nm excitation pulses of ca. 60 fs were generated by an amplified Ti:Sapphire laser system (Spectra Physics, Mountain View, CA). The transient absorption set up (Helios, Ultrafast Systems) is characterised by temporal resolution of ca. 150 fs and spectral resolution of 1.5 nm. Transient absorption data were analyzed using the Surface Xplorer PRO (Ultrafast Systems) software where it was possible to perform Singular Value Decomposition of the 3D surface into principal components (spectra and kinetics) and Global Analysis (giving lifetimes and Decay Associated Spectra (DAS) of the detected transients).[54] Target Analysis assuming several successive steps and resulting in the Species Associated Spectra (SAS)[54] was also used to globally fit the acquired data by using Glotaran.[62]

For photochemical measurements, a xenon lamp coupled with an interferential filter (λ_{exc} = 436 or 325 nm) and potassium ferrioxalate in 0.1 N sulfuric acid as actinometer were used. The occurrence of photoreactions was checked spectrophotometrically and by HPLC.

Computational details: The molecular geometries of the most stable conformer of **2** were obtained both *in vacuo* and in solution, after optimisation at Density Functional Theory (DFT)[63–66] level of theory. The 6-31+G(d) and cc–pVTZ basis sets in conjunction with the Becke three–parameter Lee–Yang–Parr (B3–LYP) hybrid exchange–correlation functional[67] and the long range corrected CAM–B3–LYP exchange-correlation functional[68] were employed. Solvent effects were taken into account by means of the implicit Conductor–like Polarisable Continuum Model (CPCM).[69,70] The solvents were chosen in order to explore a wide range of polarisation effects. The simulations were run in DCM, DCE, THF, $CHCl_3$, Ac, DMSO, MeCN, 2-PrOH, EtOH and MeOH. All the optimised geometries were also submitted to frequency calculation. The properties, frontier Kohn-Sham orbitals and excitation energies were computed for the first five singlet excited electronic states and the first five triplet excited electronic states at the Time Dependent DFT (TD–DFT) level of theory. A good agreement with experiment was found at the B3–LYP / cc–pVTZ level; no significant improvement was obtained with the long range corrected functional. The electric dipole moment **μ** and traceless quadrupole moment **Θ** were computed for the S_0 and S_1 states. Both *in vacuo* and in implicit solvents (DCM and MeCN), the S_1 state was optimised using analytical gradients,[71] and subsequently, the first transitions $S_1 \rightarrow S_0$ of the emission transition and the $S_1 \rightarrow S_n$ (n = 2, 3, 4, 5) transition energies were also simulated at TD–DFT level. The GAUSSIAN 09 computational package[72] was used for all of these calculations.

Conclusions

A comprehensive combined experimental and theoretical study allowed the deactivation dynamics of the excited states of the quadrupolar, two–branched system **2** to be clarified. The experimental findings point to a peculiar photobehaviour of **2** that shows a negative solvatochromism similar to that of the dipolar analogue **1** in absorption but also a blue shift of the emission spectrum with increasing solvent polarity that moves toward and overlaps that of compound **1** in water. The same spectral overlap was found in the S_1 state absorption spectra of of **1** and **2** in the most polar *medium*. These experimental findings point to a localisation of the excitation on one branch of the quadrupolar system, which becomes the fluorescent portion of the molecule in polar solvents and thus shows essentially the same behaviour of the corresponding single–arm compound. In fact, our theoretical results have unambiguously shown that the symmetry of the system is broken in the relaxed S_1 geometry and that a very significant charge displacement in the LUMO–HOMO molecular orbitals occurs from one branch to the other of the quadrupolar system in highly polar *media*. This work represents to the best of our knowledge the first observation of the occurrence of excited state symmetry breaking in a cationic $(D–A–D)^+$ quadrupolar system showing negative solvatochromism by a joint experimental and theoretical investigation. This latter proceeds in the direction of the advancement of the state–of–art theoretical approaches for quadrupolar systems from the present qualitative and parametrical[16,32] to quantitative QM TD–DFT models.

As for the photophysics, a strong decrease of the fluorescence in polar *media* was observed for **2**, internal conversion to the ground state becoming the unique deactivation process. In fact, femtosecond transient absorption measurements have surprisingly revealed the occurrence of a more efficient ICT in the excited states of the branched quadrupolar methyl–pyridinium derivative with respect to the dipolar analogue, particularly in the high polarity solvents. This result may provide a possible explanation for the significant NLO properties of this pyridinium compound[47] and for the observed qualitative enhancement of its TPA with respect to a dipolar analogue.[73] Another major advance is that the investigated cationic system shows a substantial solubility in water whereas in most of previous and current studies organic solvents are usually exploited, due to the very poor water solubility of the bulky quadrupolar molecules. The possibility of a comprehensive investigation of the photobehaviour in aqueous *medium* represents an added value in view of the most promising applications of the two–photon absorbing quadrupolar compounds in biology and medicine.

Acknowledgements

The authors thank the Ministero per l'Università e la Ricerca Scientifica e Tecnologica, MIUR (Rome, Italy) [PRIN "Programmi di Ricerca di Interesse Nazionale" 2010, 2010FM738P and FIRB "Futuro in Ricerca" 2010, RBFR10DAK6] and Regione Umbria (POR FSE 2007-2013, Perugia, Italy) for fundings.

The authors acknowledge the strong support and decisive advices of Prof. Ugo Mazzucato. The authors are grateful to Prof. Anna Painelli for stimulating discussions. The authors thank also Mr. Danilo Pannacci for his technical assistance in HPLC measurements and Dr. Serena Vannucci for her contributions to spectral measurements during her thesis for the first-level degree in Chemistry. The high performance computer facilities of the DreamsLab centre at the Scuola Normale Superiore are also acknowledged.

Notes and references

[a] Department of Chemistry and Centro di Eccellenza sui Materiali Innovativi Nanostrutturati (CEMIN) University of Perugia, via Elce di Sotto 8, 06123 Perugia (Italy); benedetta.carlotti@gmail.com.

[b] Scuola Normale Superiore, Collegio D'Ancona, via Consoli del Mare 15, 56126 Pisa (Italy); enrico.benassi@sns.it.

[c] Department of Chemical Sciences University of Catania, viale Andrea Doria 6, 95125 Catania (Italy).

Electronic Supplementary Information (ESI) available. See DOI: 10.1039/b000000x/

1. A. T. Yeh, C. V. Shank and J. K. McCusker, *Science*, 2000, **289**, 935.
2. S. I. Druzhinin, N. P. Ernsting, S. A. Kovalenko, L. P. Lustres, T. A. Senyushkina, and K. A. Zachariasse, *J. Phys. Chem. A*, 2006, **110**, 2955.
3. S. I. Druzhinin, S. A. Kovalenko, T. A. Senyushkina, A. Demeter, R. Machinek, M. Noltemeyer and K. A. Zachariasse, *J. Phys. Chem. A*, 2008, **112**, 8238.
4. W. Akemann, D. Laage, P. Plaza, M. M. Martin and M. Blanchard–Desce, *J. Phys. Chem. B*, 2008, **112**, 358.
5. T. Gustavsson, P. B. Coto, L. Serrano–Andrés, T. Fujiwara, and E. C. Lim, *J. Chem. Phys.*, 2009, **131**, 134312.
6. B. Carlotti, A. Spalletti, M. Šindler-Kulyk and F. Elisei, *Phys. Chem. Chem. Phys.*, 2011, **13**, 4519.
7. R. Flamini, I. Tomasi, A. Marrocchi, B. Carlotti and A. Spalletti, *J. Photochem. Photobiol. A: Chemistry,* 2011, **223**, 140.
8. B. Carlotti, R. Flamini, A. Spalletti and F. Elisei, *ChemPhysChem,* 2012, **13** (3), 724.
9. I. Kikaš, B. Carlotti, I. Škorić, M. Šindler-Kulyk, U. Mazzucato and A. Spalletti, *J. Photochem. Photobiol. A: Chemistry*, 2012, **244**, 38.
10. B. Carlotti, R. Flamini, I. Kikas, U. Mazzucato and A. Spalletti, *Chem. Phys.*, 2012, **407**, 9.
11. B. Carlotti, I. Kikaš, I. Škorić, A. Spalletti and F. Elisei, *ChemPhysChem,* 2013, **14**, 970.
12. B. Strehmel, A. M. Sarker and H. Detert, *ChemPhysChem*, 2003, **4**, 249.
13. C. Rouxel, M. Charlot, Y. Mir, C. Frochot, O. Mongin and M. Blancherd–Desce, *New J. Chem.*, 2011, **35**, 1771.
14. H. Young Woo, B. Liu, B. Kohler, D. Korystov, A. Mikhailovsky and G. C. Bazan, *J. Am. Chem. Soc.*, 2005, **127**, 14721.

15. M. Albota, D. Beljonne, J. Bredas, J. E. Ehrlich, J. Fu, A. A. Heikal, S.E. Hess, T. Kogej, M. D. Levin, S. R. Marder, D. McCord–Maughon, J. W. Perry, H. Rockel, M. Rumi, G. Subramaniam, W. W. Webb, X. Wu and C. Xu, *Science*, 1998, **281**, 1653.
16. F. Terenziani, C. Katan, E. Badaeva, S. Tretiak and M. Blanchard–Desce, *Adv. Mater.*, 2008, **20**, 4641.
17. A. Abbotto, L. Beverina, R. Bozio, A. Facchetti, C. Ferrante, G. A. Pagani, D. Pedron and R. Signorini, *Chem. Comm.* 2003, 2144.
18. M. Pawlicki, H. A. Collins, R. G. Denning and H. L. Anderson, *Angew. Chem. Int. Ed.*, 2009, **48**, 3244.
19. T. Gallavardin, C. Armagnat, O. Maury, P. L. Baldeck, M. Lindgren, C. Monnereau and C. Andraud, *Chem. Commun.*, 2012, **48**, 1689.
20. M. Velusamy, J. Shen, J. T. Lin, Y. Lin, C. Hsieh, C. Lai, M. Ho, Y. Chen, P. Chou and J. Hsiao, *Adv. Funct. Mater.*, 2009, **19**, 2388.
21. J. Trager, H. Kim and N. Hampp, *Nature Photonics*, 2007, **1**, 509.
22. K. Ogawa and Y. Kobuke, *Biomed Research International*, 2013, 125658, 1.
23. T. Gallavardin, M. Maurin, S. Marotte, T. Simon, A. Gabudean, Y. Bretonniere, M. Lindgren, F. Lerouge, P. L. Baldeck, O. Stephan, Y. Leverrier, J. Marvel, S. Parola, O. Maury and C. Andraud, *Photochem. Photobiol. Sci.*, 2011, **10**, 1216.
24. C. W. Spangler, *J. Mater. Chem.*, 1999, **9**, 2013.
25. C. Tang, Q. Zheng, H. Zhu, L. Wang, S. Chen, E. Ma and X. Chen, *J. Mater. Chem. C*, 2013, **1**, 1771.
26. C. Le Droumaguet, O. Mongin, M. H. V. Werts and M. Blanchard–Desce, *Chem. Comm.*, 2005, 2802.
27. A. Bhaskar, G. Ramakrishna, R. J. Twieg and T. Goodson III, *J. Phys. Chem. C*, 2007, **111**, 14607.
28. B. H. Cumpston, S. P. Anathavel, S. Barlow, D. L. Dyer, J. E. Ehrlich, L. L. Erskine, A. A. Heikal, S. M. Kuebler, I. Y. Sandy Lee, D. McCord–Maughon, J. Qin, H. Rockel, M. Rumi, X. Wu, S. R. Marder and J. W. Perry, *Nature*, 1999, **398**, 51.
29. Z. Li, M. Siklos, N. Pucher, K. Cicha, A. Ajami, W. Husinsky, A. Rosspeintner, E. Vauthey, G. Gescheidt, J. Stampfl and R. Liska, *J. Polymer Science Part A*, 2011, **49**, 3688.
30. Z. Li, N. Pucher, K. Cicha, J. Torgersen, S. C. Ligon, A. Ajami, W. Husinsky, A. Rosspeintner, E. Vauthey, S. Naumov, T. Scherzer, J. Stampfl and R. Liska, *Macromolecules*, 2013, **46**, 352.
31. K. Susumu, J. A. N. Fisher, J. Zheng, D. N. Beratan, A. G. Yodh and M. J. Therien, *J. Phys. Chem. A*, 2011, **115**, 5525.
32. F. Terenziani, A. Painelli, C. Katan, M. Charlot and M. Blanchard–Desce, *J. Am. Chem. Soc.*, 2006, **128**, 15742.
33. A. Bhaskar, G. Ramakrishna, Z. Lu, R. Twieg, J. M. Hales, D. J. Hagan, E. Van Stryland and T. Goodson III, *J. Am. Chem. Soc.*, 2006, **128**, 11840.
34. G. Ramakrishna and T. Goodson III, *J. Phys Chem A*, 2007, **111**, 993.
35. P. D. Zoon, I. H. M. van Stokkum, M. Parent, O. Mongin, M. Blanchard–Desce and A. M. Brouwer, *Phys. Chem. Chem. Phys.*, 2010, **12**, 2706.
36. E. Vauthey, *Chem. Phys. Chem*, 2012, **13**, 2001.
37. F. Terenziani, O. V. Przhonska, S. Webster, L. A. Padilha, Y. L. Slominsky, I. G. Davydenko, A. O. Gerasov, Y. P. Kovtun, M. P. Shandura, A. D. Kachovski, D. J. Hagan, E. W. Van Stryland and A. Painelli, *J. Phys. Chem. Lett.,* 2010, **1**, 1800.
38. H. Hu, O. V. Przhonska, F. Terenziani, A. Painelli, D. Fishman, T. R. Ensley, M. Reichert, S. Webster, J. L. Bricks, A. D. Kachkovski, D. J. Hagan and E. W. Van Stryland, *Phys. Chem. Chem. Phys.*, 2013, **15**, 7666.
39. R. Ramadass and J. Bereiter–Hajn, *J. Phys. Chem. B,* 2007, **111**, 7681.
40. B. Carlotti, C. G. Fortuna, G. Consiglio, U. Mazzucato, A. Spalletti and F. Elisei, *J. Phys. Chem. A*, DOI: 10.1021/jp407342q.
41. N. A. Nemkovich, H. Detert and V. Schmitt, *Chem. Phys.*, 2010, **378**, 37.
42. Z. R. Grabowski, K. Rotkiewicz, and W. Rettig, *Chem. Rev.*, 2003, **103**, 3899.
43. R. A. Marcus, *J. Phys. Chem.*, 1989, **93**, 3078.
44. C.L. Zhang and D. Y. Wang, *J. Photochem. Photobiol. A: Chem.*, 2002, **147**, 93.
45. M. Matsui, S. Kawamura, K. Shibata and H. Muramatsu, *Bull. Chem. Soc. Japan,* 1992, **65,** 71.
46. H. Wang, R. Helgeson, B. Ma and F. Wudl, *J. Org. Chem.*, 2000, **65**, 5862.
47. X. Xu, W. Qiu, Q. Zhou, J. Tang, F.Yang, Z. Sun and P. Audebert, *J. Phys. Chem. B,* 2008, **112,** 4913.
48. D. Laage, W.H.Thompson, M. Blanchard-Desce, and J. T. Hines, *J. Phys. Chem. A*, 2003, **107**, 6032.
49. R. Daudel, R. Lefebvre, and C. Moser, *Quantum Chemistry. Methods and Applications*, Interscience Publishers Inc., New York, **1959**, Cap. IX.
50. P. Fromherz, *J. Phys. Chem.*, 1995, **99**, 7188.
51. N. Ghoneim and P. Suppan, *Spectrochimica Acta*, 1995, **51A** (6), 1043.
52. D. Jacquemin, E. A. Perpete, I. Ciofini and C. Adamo, *Acc. Chem. Res.* 2009, **42**, 326.
53. V. Barone, A. Baiardi, M. Biczisko, J. Bloino, C. Cappelli and F. Lipparini, *Phys. Chem. Chem. Phys.,* 2012, **14**, 12404.
54. I.H.M. van Stokkum, D.S. Larsen and R. van Grondelle, *Biochim. Biophys. Acta*, 2004, **1657**, 82.
55. M. L. Horng, J. A. Gardecki, A. Papazyan and M. Maroncelli, *J. Phys. Chem.*, 1995, **99**, 17311.
56. H. Wang, H. Zhang, W. Rettig, A. I. Tolmachev, and M. Glasbeek, *Phys. Chem. Chem. Phys.*, 2004, **6**, 3437.
57. G. C. Fortuna, V. Barresi, C. Bonaccorso, G. Consiglio, S. Failla, A. Trovato–Salinaro and G. Musumarra, *Eur. J. Med. Chem.,* 2012, **47**, 221 and references therein.
58. H. Görner, F. Elisei and G.G. Aloisi, *J. Chem. Soc., Faraday Trans.,* 1992, **88**, 29.
59. A. Romani, F. Elisei, F. Masetti and G. Favaro, *J. Chem. Soc., Faraday Trans.,*1992, **88**, 2147.

60. B. Carlotti, D. Fuoco and F. Elisei, *Phys. Chem. Chem. Phys.,*2010, **12**,15580.
61. B. Carlotti, A. Cesaretti and F. Elisei *Phys. Chem. Chem. Phys.,* 2012, **14**, 823.
62. Copyright © 2009, J. Snellenburg, VU University Amsterdam; http://glotaran.org/
63. P. Hohenberg and W. Kohn, *Phys. Rev*., 1964,**136**, B864.
64. W. Kohn and L. J. Sham, *Phys. Rev*., 1965,**140**, A1133.
65. D. R. Salahub and M. C. Zerner, (Eds.) *The Challenge of d and f Electrons*; ACS: Washington, D.C., 1989.
66. R. G. Parr and W. Yang, *Density-functional theory of atoms and molecules*; Oxford University Press: Oxford, 1989.
67. A. D. Becke, *J. Chem. Phys.,*1993, **98**, 5648.
68. T. Yanai, D. Tew and N. Handy, *Chem. Phys. Lett.* 2004, **393**, 51.
69. V. Barone and M. Cossi, *J. Phys. Chem. A*, 1998, **102**, 1995.
70. M. Cossi, N. Rega, G. Scalmani and V. Barone, *J. Comp. Chem.,* 2003, **24**, 669.
71. G. Scalmani, M. J. Frisch, B. Mennucci, J. Tomasi, R. Cammi and V. Barone, *J. Chem. Phys*., 2006, **124**, 094107 1.
72. *GAUSSIAN 09*, *Revision C.01*, M. J. Frisch, G. W. Trucks, H. B. Schlegel, G. E. Scuseria, M. A. Robb, J. R. Cheeseman, G. Scalmani, V. Barone, B. Mennucci, G. A. Petersson, H. Nakatsuji, M. Caricato, X. Li, H. P. Hratchian, A. F. Izmaylov, J. Bloino, G. Zheng, J. L. Sonnenberg, M. Hada, M. Ehara, K. Toyota, R. Fukuda, J. Hasegawa, M. Ishida, T. Nakajima, Y. Honda, O. Kitao, H. Nakai, T. Vreven, J. A. Montgomery, Jr., J. E. Peralta, F. Ogliaro, M. Bearpark, J. J. Heyd, E. Brothers, K. N. Kudin, V. N. Staroverov, R. Kobayashi, J. Normand, K. Raghavachari, A. Rendell, J. C. Burant, S. S. Iyengar, J. Tomasi, M. Cossi, N. Rega, J. M. Millam, M. Klene, J. E. Knox, J. B. Cross, V. Bakken, C. Adamo, J. Jaramillo, R. Gomperts, R. E. Stratmann, O. Yazyev, A. J. Austin, R. Cammi, C. Pomelli, J. W. Ochterski, R. L. Martin, K. Morokuma, V. G. Zakrzewski, G. A. Voth, P. Salvador, J. J. Dannenberg, S. Dapprich, A. D. Daniels, O. Farkas, J. B. Foresman, J. V. Ortiz, J. Cioslowski, and D. J. Fox, Gaussian, Inc., Wallingford CT, 2009.
73. F. Hao, P. Shi, H. Liu, J. Wu, J. Yang, Y. Tian, G. Zhou, M. Jiang, H. Fun and C. Suchada, *Chinese J. Chem.*, 2004, **22**, 354.